

# Quantum communication through anisotropic Heisenberg XY spin chains

Z.-M. Wang<sup>a,b</sup> M. S. Byrd<sup>a,c</sup> B. Shao<sup>b</sup> J. Zou<sup>b</sup>

<sup>a</sup>*Department of Physics, Southern Illinois University, Carbondale, Illinois 62901-4401*

<sup>b</sup>*Department of Physics, Beijing Institute of Technology, Beijing, 100081*

<sup>c</sup>*Department of Computer Science, Southern Illinois University, Carbondale, Illinois 62901-4401*

---

## Abstract

We study quantum communication through an anisotropic Heisenberg XY chain in a transverse magnetic field. We find that for some time  $t$  and anisotropy parameter  $\gamma$ , one can transfer a state with a relatively high fidelity. In the strong-field regime, the anisotropy does not significantly affect the fidelity while in the weak-field regime the affect is quite pronounced. The most interesting case is the the intermediate regime where the oscillation of the fidelity with time is low and the high-fidelity peaks are relatively broad. This would, in principle, allow for quantum communication in realistic circumstances. Moreover, we calculate the purity, or tangle, as a measure of the entanglement between one spin and all the other spins in the chain and find that the stronger the anisotropy and exchange interaction, the more entanglement will be generated for a given time.

*Key words:* Quantum State Transfer, Entanglement

*PACS:* 03.67Hk, 03.65Ud, 75.10Jm

---

## 1 Introduction

The transfer of a quantum state from one place to another is an important task in quantum information processing. A quantum state prepared by one party needs to be measured by another party at a distance. Long distance

---

*Email addresses:* mingmoon78@126.com (Z.-M. Wang), mbyrd@physics.siu.edu (M. S. Byrd).

communication between two parties, for example, in quantum key distribution [1], can be realized by means of photons. In this case, photons have the advantage that they have an extremely small interaction with the environment and also travel long distances quickly through optical fibers or empty space. However, for short distance communication, such as connecting distinct quantum processors or registers inside a quantum computer [2,3], conditions and requirements are different [4]. Recently, quantum communication through spin chains has been intensively investigated for this purpose [5,6,7].

The primary scheme is that one quantum state is produced at one end of the chain; it evolves naturally under spin chain dynamics; and at some time  $t$  we receive the state at the other end [5]. For more complex systems, Christandl et al. suggested a perfect state transfer algorithm which can transfer an arbitrary quantum state between two ends of a spin chain [6], or a more complex spin network [7]. In addition, researchers have investigated measurement-assisted optimal quantum communication by a single chain [8] and parallel chain [9,10], the entanglement transfer through a Heisenberg XY chain [11,12] and parallel spin chains [13], enhancement of state transfer with energy current [14] and entanglement transfer by phase control [15,16]. However, due to the complexity of the problem researchers usually consider cases where the magnetization ( $z$  component of the total spin  $\sum_i S_i^z$ ) is a conserved quantity, which means that  $[\sum_i S_i^z, H] = 0$ . For the cases that the Hamiltonian does not satisfy above conditions, L. Amico et al. studied the dynamics of entanglement and found that the anisotropy of the Hamiltonian has an evident effect on the evolution of entanglement [17,18]. They calculated the entanglement using the out-of-equilibrium correlation functions, but did not investigate state transfer in these systems. The anisotropy and magnetic field effects on the entanglement transfer in two parallel Heisenberg spin chains was later investigated in Ref. [19]. For the simple cases where each chain only has two spins, it was determined that perfect entanglement transfer can be realized between spin pairs by adjusting the magnetic field strength and the anisotropy parameter.

In this paper, we study quantum communication in an anisotropic Heisenberg XY chain with small number of particles  $N$  and an arbitrary initial state. Following the scenario of earlier work on state transfer through spin chains, we encode a state to be transferred at the first site of the chain and, without external control, let the chain freely evolve. After time  $t$  the state is to be readout at the  $r^{\text{th}}$  site of the chain. But different from the other cases with  $[\sum_i S_i^z, H] = 0$ , the quantum communication channel, the spin chain, not only transfers the state, but also generates entanglement.

This paper is organized as follows: In part two we will give our model Hamiltonian and calculate the time dependence of the one-site correlation function which will be used in the expression of the fidelity and tangle. In part three, we discuss the time evolution of transmission fidelity and purity in a short

chain for three regimes: strong-field, weak-field and intermediate regime. The final part is devoted to the conclusions.

## 2 The model and the calculation

The Hamiltonian of the anisotropic Heisenberg XY chain in a uniform transverse magnetic field  $h$  is given by [20]

$$H = - \sum_{i=1}^N (J^x S_i^x S_{i+1}^x + J^y S_i^y S_{i+1}^y) - \sum_{i=1}^N h S_i^z. \quad (1)$$

where  $S_i^a$  is the  $a$  spin operator ( $a = x, y, z$ ) at site  $i$ ,  $J^x$  and  $J^y$  are the anisotropic exchange interaction constants, and  $h$  is the transverse magnetic field. We assume periodic boundary conditions, so that the  $N^{\text{th}}$  site is identified with the  $0^{\text{th}}$  site. The standard procedure used to solve Eq. (1) is to transform the spin operators  $S_i^a$  into fermionic operators via the Jordan-Wigner(J-W) transformation

$$c_1 = S_1^-, c_n = (-2S_1^z)(-2S_2^z) \cdots (-2S_{n-1}^z) S_n^-, n = 2, \dots, N, \quad (2)$$

where  $c_n$  are one-dimensional spinless fermions annihilation operators and  $S_1^- = S_1^x - iS_1^y$ .

It will be convenient to introduce operators  $A_l = c_l^\dagger + c_l$ , and  $B_l = c_l^\dagger - c_l$ , which fulfill the anti-commutation relations

$$\{A_l, A_m\} = -\{B_l, B_m\} = 2\delta_{lm}, \quad \{A_l, B_m\} = 0, \quad (3)$$

In terms of these operators, the J-W transformation reads

$$S_l^x = \frac{1}{2} A_l \prod_{s=1}^{l-1} A_s B_s, \quad S_l^y = -\frac{i}{2} B_l \prod_{s=1}^{l-1} A_s B_s, \quad S_l^z = -\frac{1}{2} A_l B_l, \quad (4)$$

Using the J-W transformation, Eq. (1) becomes the bi-linear form

$$H = - \sum_i \left\{ \frac{J}{2} \left[ (c_i^\dagger c_{i+1} - c_i c_{i+1}^\dagger) + \gamma (c_i^\dagger c_{i+1}^\dagger - c_i c_{i+1}) \right] + h \left( c_i^\dagger c_i - \frac{1}{2} \right) \right\}. \quad (5)$$

where  $J = \frac{1}{2}(J^x + J^y)$ , and  $\gamma = (J^x - J^y)/(J^x + J^y)$  is the anisotropy parameter. The limiting values,  $\gamma = 0$  and  $1$  correspond to the isotropic and Ising chain, respectively.

Eq. (5) can be diagonalized by the transformation [17,18]

$$\eta_k = \frac{1}{\sqrt{N}} \sum_l e^{ikl} (\alpha_k c_l + i\beta_k c_l^\dagger), \quad (6)$$

where

$$\begin{aligned}\alpha_k &= \sqrt{\frac{1 - (h + J \cos k)/\lambda_k}{2}}, \\ \beta_k &= \text{sign}(J\gamma \sin k) \sqrt{\frac{1 + (h + J \cos k)/\lambda_k}{2}}, \\ \lambda_k &= \sqrt{(h + J \cos k)^2 + J^2 \gamma^2 \sin^2 k},\end{aligned}\tag{7}$$

The Hamiltonian in Eq. (5) then becomes

$$H = \sum_k \lambda_k \left( \eta_k^\dagger \eta_k - \frac{1}{2} \right).\tag{8}$$

where the wave number  $k = 2\pi m/N$  with  $-N/2 < m \leq N/2$ .

Now that the  $XY$  Hamiltonian has been diagonalized, we will calculate the evolution of the operators  $c_j^\dagger, c_j$ , which will be used to obtain the final state. From Eq. (6) and its inverse

$$c_j(t) = \frac{1}{\sqrt{N}} \sum_k e^{-ikj} (\alpha_k \eta_k(t) - i\beta_k \eta_{-k}^\dagger(t)),\tag{9}$$

where  $\eta_k(t) = e^{-i\lambda_k t} \eta_k(0)$ .

Then from Eqs. (6) and (9)

$$\begin{aligned}c_j(t) &= \sum_l [\tilde{a}_{lj}(t) c_l + \tilde{b}_{lj}(t) c_l^\dagger], \\ c_j^\dagger(t) &= \sum_l [\tilde{b}_{lj}^\dagger(t) c_l + \tilde{a}_{lj}^\dagger(t) c_l^\dagger],\end{aligned}\tag{10}$$

where

$$\begin{aligned}\tilde{a}_{lj}(t) &= \frac{1}{N} \sum_k e^{ik(l-j)} [e^{i\lambda_k t} - 2i\alpha_k^2 \sin \lambda_k t], \\ \tilde{b}_{lj}(t) &= \frac{2}{N} \sum_k e^{ik(l-j)} \alpha_k \beta_k \sin \lambda_k t.\end{aligned}\tag{11}$$

For  $\gamma = 0$ , and  $\alpha_k = 0$ , the evolution of the creation operator is

$$c_j^\dagger(t) = \frac{1}{N} \sum_l e^{-ik(l-j)} e^{-i\lambda_k t} c_l^\dagger.$$

In this case the  $z$ -component of the total spin  $S^z$  commutes with the Hamiltonian and is a conserved quantity.

Now we seek to transfer a quantum state from the site  $s$  to  $r$ . First we assume that all the spins of the system are initially in spin down states. Then we encode the state  $|\varphi(0)\rangle = \alpha|0\rangle + \beta|1\rangle$  at the first spin of the chain. The initial state of the whole system is then  $|\Phi(0)\rangle = (\alpha + \beta c_1^\dagger)|\mathbf{0}\rangle$ , where  $|\mathbf{0}\rangle$  denotes the state with all the spins down. For simplicity,  $\alpha$  and  $\beta$  are taken to be real with  $\alpha^2 + \beta^2 = 1$ . Now our task is to calculate the fidelity of transmission of a state from the first spin to the  $r^{\text{th}}$  spin of the chain.

The reduced density matrix of the  $r^{\text{th}}$  spin of the chain can be constructed using the operator expansion for the density matrix of a system on  $N$  spin-1/2 particles in terms of tensor products of Pauli matrices. The reduced density matrix is [21]

$$\rho_r(t) = \begin{pmatrix} \frac{1}{2} + \langle S_r^z \rangle & \langle S_r^x \rangle - i \langle S_r^y \rangle \\ \langle S_r^x \rangle + i \langle S_r^y \rangle & \frac{1}{2} - \langle S_r^z \rangle \end{pmatrix}. \quad (12)$$

where  $\langle S_r^{x,y,z} \rangle$  means  $\langle \Phi(0) | S_r^{x,y,z} | \Phi(0) \rangle$ .

The fidelity between the received state  $\rho_r(t)$  and the initial state  $\varphi(0)$  is defined by  $F = \sqrt{\langle \varphi(0) | \rho_r(t) | \varphi(0) \rangle}$  which is

$$F = \sqrt{\frac{1}{2} + (\beta^2 - \alpha^2) \langle S_r^z \rangle + 2\alpha\beta \langle S_r^x \rangle}. \quad (13)$$

So if the parameters  $\alpha = \beta = 1/\sqrt{2}$ , the fidelity  $F = \sqrt{\frac{1}{2} + \langle S_r^x \rangle}$ , which only depends on the value of  $\langle S_r^x \rangle$ .

Another quantity we want to calculate is the purity (also known as the tangle or one-tangle), which provides a measure of the entanglement between the spin at one site and the rest of sites in the chain. The purity is often expressed as  $1 - \text{Tr}(\rho^2)$ , but can also be expressed as

$$\tau[\rho^{(1)}] = 4 \det[\rho^{(1)}], \quad (14)$$

where  $\rho^{(1)}$  is the one-site reduced density matrix, Eq. (12). This is referred to as the one-tangle [18], which was apparently motivated by the tangle defined in Ref. [22]. Note that Eq. (14) gives a valid measure of entanglement when the whole system is in a pure state and given there is only one parameter for a any such measure for a two-state system, this is as good as any other. However, if the system is in a mixed state, one must use some other measure of entanglement. The one-tangle, or purity, is connected to the Von Neumann entropy of the reduced density matrix through the relation

$$S[\rho^{(1)}] = h\left(\frac{1}{2}(1 + \sqrt{1 - \tau[\rho^{(1)}]})\right), \quad (15)$$

where  $h(x) = -x \log_2 x - (1-x) \log_2 (1-x)$ . From Eq. (12), the tangle/purity

can be written as

$$\tau[\rho^{(1)}] = 4 \det[\rho^{(1)}] = 1 - 4(\langle S_r^x \rangle^2 + \langle S_r^y \rangle^2 + \langle S_r^z \rangle^2), \quad (16)$$

where the components  $S^\alpha$  are the components of the Bloch vector.

Now we will calculate  $\langle S_r^a(t) \rangle$  ( $a = x, y, z$ ) for use in Eqs. (13) and (16) .

$$\langle S_r^x(t) \rangle = \alpha^2 \langle \mathbf{0} | S_r^x(t) | \mathbf{0} \rangle + \beta^2 \langle \mathbf{1} | S_r^x(t) | \mathbf{1} \rangle + \alpha\beta(\langle \mathbf{0} | S_r^x(t) | \mathbf{1} \rangle + \langle \mathbf{1} | S_r^x(t) | \mathbf{0} \rangle). \quad (17)$$

However, note that  $\langle \mathbf{0} | S_r^x(t) | \mathbf{0} \rangle = \langle \mathbf{1} | S_r^x(t) | \mathbf{1} \rangle = 0$ .

Using Wick's theorem,

$$\begin{aligned} \langle S_r^x(t) \rangle = \frac{1}{2} \alpha \beta \{ & \langle \mathbf{0} | (A_1 c_1^\dagger + c_1 A_1) | \mathbf{0} \rangle \langle \mathbf{0} | B_1 A_2 B_2 \dots A_{r-1} B_{r-1} A_r | \mathbf{0} \rangle - \\ & \langle \mathbf{0} | (B_1 c_1^\dagger + c_1 B_1) | \mathbf{0} \rangle \langle \mathbf{0} | A_1 A_2 B_2 \dots A_{r-1} B_{r-1} A_r | \mathbf{0} \rangle + \\ & \dots + \langle \mathbf{0} | (A_r c_1^\dagger + c_1 A_r) | \mathbf{0} \rangle \langle \mathbf{0} | A_1 B_1 A_2 B_2 \dots A_{r-1} B_{r-1} | \mathbf{0} \rangle \}. \end{aligned} \quad (18)$$

For the simple case,  $N = 3$ ,  $r = 2$

$$\begin{aligned} \langle S_r^x(t) \rangle = \frac{\alpha\beta}{2} \{ & \langle \mathbf{0} | (A_1 c_1^\dagger + c_1 A_1) | \mathbf{0} \rangle \langle \mathbf{0} | B_1 A_2 | \mathbf{0} \rangle \\ & - \langle \mathbf{0} | (B_1 c_1^\dagger + c_1 B_1) | \mathbf{0} \rangle \langle \mathbf{0} | A_1 A_2 | \mathbf{0} \rangle \\ & + \langle \mathbf{0} | (A_2 c_1^\dagger + c_1 A_2) | \mathbf{0} \rangle \langle \mathbf{0} | A_1 B_1 | \mathbf{0} \rangle \}. \end{aligned} \quad (19)$$

The value of  $\langle S_r^y \rangle$  can be obtained from the above expression by replacing  $A_r \rightarrow B_r$  and  $1/2 \rightarrow -i/2$ .

Now we need to calculate *contractions* of two field operators  $\langle \mathbf{0} | A_j B_m | \mathbf{0} \rangle$ ,  $\langle \mathbf{0} | A_j A_m | \mathbf{0} \rangle$ ,  $\langle \mathbf{0} | B_j B_m | \mathbf{0} \rangle$ ,  $\langle \mathbf{0} | B_j A_m | \mathbf{0} \rangle$ . From Eqs. (10)- (11), we get

$$\begin{aligned}
\langle \mathbf{0} | A_j(t) B_m(t) | \mathbf{0} \rangle &= \delta_{jm} \\
&\quad - \frac{4}{N} \sum_k [2\alpha_k^2 \beta_k^2 \cos k(j-m) \\
&\quad + \alpha_k \beta_k (1 - 2\beta_k^2) \sin k(j-m)] \sin^2 \lambda_k t \\
&\quad + \frac{2}{N} \sum_k \alpha_k \beta_k \cos k(j-m) \sin 2\lambda_k t,
\end{aligned} \tag{20}$$

$$\begin{aligned}
\langle \mathbf{0} | A_j(t) A_m(t) | \mathbf{0} \rangle &= \delta_{jm} \\
&\quad - \frac{4i}{N} \sum_k [\alpha_k \beta_k (1 - 2\alpha_k^2) \cos k(j-m) \\
&\quad - 2\alpha_k^2 \beta_k^2 \sin k(j-m)] \sin^2 \lambda_k t \\
&\quad + \frac{2i}{N} \sum_k \alpha_k \beta_k \sin k(j-m) \sin 2\lambda_k t,
\end{aligned} \tag{21}$$

$$\begin{aligned}
\langle \mathbf{0} | B_j(t) B_m(t) | \mathbf{0} \rangle &= -\delta_{jm} \\
&\quad - \frac{4i}{N} \sum_k [\alpha_k \beta_k (1 - 2\alpha_k^2) \cos k(j-m) \\
&\quad + 2\alpha_k^2 \beta_k^2 \sin k(j-m)] \sin^2 \lambda_k t \\
&\quad + \frac{2i}{N} \sum_k \alpha_k \beta_k \sin k(j-m) \sin 2\lambda_k t.
\end{aligned} \tag{22}$$

and

$$\begin{aligned}
\langle \mathbf{0} | A_j(t) c_1^\dagger + c_1 A_j(t) | \mathbf{0} \rangle &= \frac{2}{N} \sum_k [\cos k(1-j) \cos \lambda_k t \\
&\quad - (1 - 2\alpha_k^2) \sin k(1-j) \sin \lambda_k t \\
&\quad + 2\alpha_k \beta_k \cos k(1-j) \sin \lambda_k t],
\end{aligned} \tag{23}$$

$$\begin{aligned}
\langle \mathbf{0} | B_j(t) c_1^\dagger + c_1 B_j(t) | \mathbf{0} \rangle &= \frac{-2i}{N} \sum_k [(1 - 2\alpha_k^2) \cos k(1-j) \sin \lambda_k t \\
&\quad + \sin k(1-j) \cos \lambda_k t \\
&\quad + 2\alpha_k \beta_k \sin k(1-j) \sin \lambda_k t].
\end{aligned} \tag{24}$$

Now we can calculate  $\langle S_r^z \rangle$

$$\langle S_r^z \rangle = -\frac{1}{2} [\alpha^2 \langle \mathbf{0} | A_r B_r | \mathbf{0} \rangle + \beta^2 \langle \mathbf{1} | A_r B_r | \mathbf{1} \rangle + \alpha\beta (\langle \mathbf{0} | A_r B_r | \mathbf{1} \rangle + \langle \mathbf{1} | A_r B_r | \mathbf{0} \rangle)]. \tag{25}$$

Note that, since  $\langle \mathbf{0} | A_r B_r | \mathbf{1} \rangle = \langle \mathbf{1} | A_r B_r | \mathbf{0} \rangle = 0$ , then  $\langle \mathbf{0} | A_r(t) B_r(t) | \mathbf{1} \rangle = \langle \mathbf{1} | A_r(t) B_r(t) | \mathbf{0} \rangle = 0$  [18],

$$\langle S_r^z \rangle = -\frac{1}{2} \left[ \langle \mathbf{0} | A_r B_r | \mathbf{0} \rangle + \beta^2 \left( |\tilde{b}_{1r}|^2 - |\tilde{a}_{1r}|^2 \right) \right]. \tag{26}$$

Now, from Eq. (20),  $\langle \mathbf{0} | A_r B_r | \mathbf{0} \rangle = 1 - \frac{8}{N} \sum_k \alpha_k^2 \beta_k^2 \sin^2 \lambda_k t$ .

For the case  $\gamma = 0$ ,  $\alpha_k = 0$ , we find that

$$\langle S_r^x(t) \rangle = \frac{\alpha\beta}{N} \sum_k \cos[k(r-1) - \lambda_k t], \quad \langle S_r^z \rangle = \beta^2 |\tilde{a}_{1r}|^2 - \frac{1}{2}. \quad (27)$$

which agrees with Bose's case [5]. The  $\tilde{a}_{1r}$  gives the transmission amplitude  $f_{rs}^N(t)$  of an excitation (the  $|1\rangle$  state) from the 1<sup>st</sup> to the  $r^{\text{th}}$  spin. When  $\alpha = \beta = 1/\sqrt{2}$ , the fidelity is

$$F = \sqrt{\frac{1}{2} + \frac{1}{2} \frac{1}{N} \sum_k \cos[k(r-1) - \lambda_k t]}. \quad (28)$$

which agrees with Ref. [14].

### 3 Results and discussion: Fidelity of state transfer

We will now investigate the performance of a spin chain for which there exists some anisotropy parameter  $\gamma$  and the  $z$ -component of the total spin is not a conserved quantity. We first perform numerical calculations of the fidelity  $F$  for a particular, and small  $N$  value and discuss the variations with changes in physical properties of the system.

As stated above, after some time  $t$ , the state at the  $r^{\text{th}}$  spin will be measured, where  $r = N/2 + 1$  for  $N$  even and  $r = (N+1)/2 + 1$  for  $N$  odd, i.e. the sending and receiving positions are at opposite sites on the chain with periodic boundary conditions. Clearly the complexity of the computation grows with the value of  $r$  because the expansion of  $\langle S_r^x(t) \rangle$  has  $(2r-1)!!$  terms. So for simplicity, we take  $N = 5$ ,  $r = 3$  as an example. We will also choose a particular state  $(\sqrt{3}/2 |0\rangle + 1/2 |1\rangle)$  to analyze. However, it is important to note that we have examined several states and have found these trends typical; they exhibit similar variations, only the maximal values of the fidelity and purity/tangle are different. In each case the final state Eq. (12) has a time dependence described by Eqs. (17) and (25). The state to be transferred is encoded at the first site of the chain. Then as time evolves the state propagates to the  $r^{\text{th}}$  site. The time evolution of the operators  $\langle S_r^a(t) \rangle$  ( $a = x, y, z$ ) can be expressed as a product of all contractions of the two operators  $A(t)$  and  $B(t)$ , which are superpositions of many different states in the basis spanned by the Jordan-Wigner fermions with definite momenta [23]. This is clearly more complex than the isotropic case ( $\gamma = 0$ ) where the state transfer can be characterized in terms of their dispersion [5].



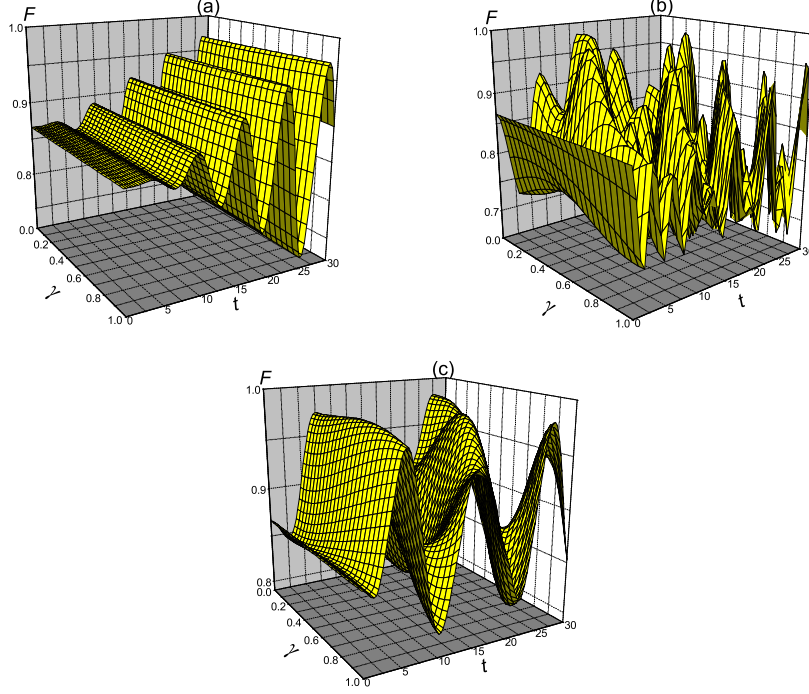


Fig. 1. The fidelity  $F$  is plotted versus time  $t$  and anisotropic parameter  $\gamma$  for (a) Strong-field regime,  $h = 1.0$ ,  $J = 0.1$ . (b) Weak-field regime,  $h = 0.1$ ,  $J = 1.0$ . (c) Intermediate case,  $h = J = 0.5$ . The number of sites  $N$  is 5, the input state is encoded in the first site and output state is at the 3<sup>rd</sup> site,  $\alpha = \sqrt{3}/2, \beta = 1/2$ .

### 3.1 The strong-field regime

The fidelity  $F$  as a function of time  $t$  and the anisotropic parameter  $\gamma$  are shown in Fig. 1 with different parameter values for  $J$  and  $h$ . First in the strong-field regime (Fig. 1(a)),  $J/h \ll 1$ , the dispersion is given by  $\lambda_k = h[1 + (J/h) \cos k + (J/h)^2(\cos^2 k + \gamma^2 \sin^2 k)/2 + o((J/h)^3)]$ . The effect of the anisotropy can be neglected if we only consider the term which is first order in  $J/h$ . The parameters in Eq. (7) become  $\alpha_k \rightarrow 0, \beta_k \rightarrow \pm 1$  and  $\tilde{b}_{lj} \rightarrow 0$  in Eq. (11). So the contractions of two field operators in Eqs. (20)- (22) are negligible for  $j \neq m$  which indicates that using only a uniform magnetic field (global interaction) cannot cause a uncorrelated state to become correlated. In Fig. 1(a), it is clear that the anisotropy does not significantly affect the fidelity, but the presence of the cosine term in the first order of the dispersion produces the observed oscillation of fidelity with time  $t$ .

### 3.2 The weak-field regime

In the weak-field regime  $h/J \ll 1$  (Fig. 1(b)), the dispersion can be written as  $\lambda_k = J[2(h/J) \cos k + (h/J)^2 + \cos^2 k + \gamma^2 \sin^2 k]^{1/2}$ . In this case, the anisotropy has pronounced effects on the fidelity. We see that increasing the anisotropy does not always decrease the fidelity. For certain values of the parameters  $\gamma$  and  $t$ , the fidelity is greater, which corresponds to a constructive interference. For example, there are peaks with  $\gamma \neq 0$  such as  $(\gamma = 0.28, t = 27.70, F = 0.98)$  and  $(\gamma = 0.42, t = 7.10, F = 0.98)$  that exhibit this behavior. With increasing  $\gamma$  and  $t$ , the frequency of oscillation of  $F$  becomes greater. The higher-frequency oscillation can be attributed to the fact that with increasing  $\gamma$  the initial state differs more from the true ground state, and therefore, with the evolution of time, it exhibits fluctuations, even near the ground state.

### 3.3 The intermediate regime

The intermediate regime ( $J \sim h$ ), which is the most interesting, is shown in Fig. 1(c). For relatively short times  $0 < t < 10$ , the anisotropy does not have a pronounced effect on the fidelity. The oscillation of  $F$  with time  $t$  is relatively slow in this case compared to the cases in both the strong- and weak-field regimes, Fig. 1(a) and (b) respectively. When the strength of the exchange interaction  $J$  or the magnetic field  $h$  dominate, the oscillation of  $F$  with time  $t$  is greater. But for intermediate regimes, the competition between  $J$  and  $h$  gives a smaller oscillation frequency for  $F$ . Furthermore, the high-fidelity peaks are fairly broad and therefore correspond to values of the fidelity which are stable under perturbation of the parameters.

### 3.4 Comparison

In summary, realistic quantum communication devices will require larger fidelities in a shorter times. One may well have expected a significant oscillation of fidelity with time and anisotropy in the intermediate regime. However, this is not the case, but rather the intermediate regime has the highest fidelities in the shortest amount of time with the more stable values for the fidelity. So if one wants to achieve the highest fidelity under our assumed conditions, the intermediate regime is, surprisingly, the best choice.

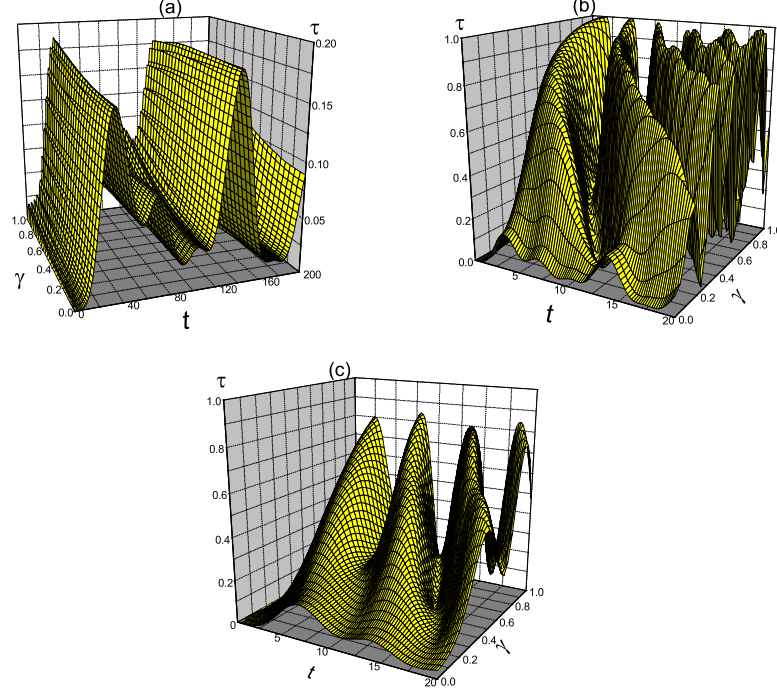


Fig. 2. The one-tangle, or purity, at the 3<sup>rd</sup> site as a function of time  $t$  and  $\gamma$ . The initial state of the system is  $(\sqrt{3}/2 |0\rangle + 1/2 |1\rangle) \otimes |0\rangle$ . (a) Strong-field regime,  $h = 1.0, J = 0.1$ . (b) Weak-field regime,  $h = 0.1, J = 1.0$ . (c) Intermediate regime,  $h = J = 0.5$ .

#### 4 Results and discussion: Entanglement

It is clear that the initial state of the system is an unentangled state. However, with the evolution of time, entanglement is generated in the chain. In order to quantify this change, we have calculated the purity, or tangle, at the 3<sup>rd</sup> site which measures the entanglement between the 3<sup>rd</sup> site and all the other sites in the chain. The tangle at 3<sup>rd</sup> site as a function of time  $t$  and anisotropy  $\gamma$  is plotted in Fig. 2 and Fig. 3 with different initial states  $(\alpha |0\rangle + \beta |1\rangle) \otimes |0\rangle$  and vacuum state, respectively. From Fig. 2, for small anisotropy ( $\gamma < 0.1$ ), the tangle is negligibly small. In the strong-field regime, from Fig. 3(a), the anisotropy does not have a significant affect on the tangle similar to behaviour of the fidelity as seen in Fig. 2(a). Also, the strong-field tangle is relatively small compared to the weak-field regime and the oscillation of tangle with time  $t$  is suppressed. Furthermore, the time for the tangle reach its first peak in the strong-field regime is at  $t \approx 45$  while for the intermediate regime it is  $t \approx 5$ .

In the weak-field regime, which is plotted in Fig. 2(b) and Fig. 3(b), we see that a stronger exchange interaction even with a stronger anisotropy can generate more entanglement at certain times. For example, at  $\gamma = 1.0$  and  $t = 1.5$ ,

$\tau = 1.0$ .

In the intermediate regime, the behaviour of the tangle is similar to the weak-field regime. With increasing anisotropy, the tangle increases. However, even in the  $\gamma = 1.0$  case, it does not reach its maximal value  $\tau = 1.0$ . Also, as  $J/h$  increases, the tangle oscillates more rapidly, but different from the effect of anisotropy on fidelity in the intermediate case, (see Fig. 2(b)) the tangle increases with increasing  $\gamma$ . This is an effect of entanglement dynamically generated from the ground state and depends on the anisotropy. When the initial state is the ground state, the system will still generate entanglement, which exists only in the  $\gamma \neq 0$  case. This is due to the double spin-flip operator terms  $\gamma(c_i^\dagger c_{i+1}^\dagger - c_i c_{i+1})$  in Eq. (5). In this case,  $\langle \mathbf{0} | S_r^x(t) | \mathbf{0} \rangle = \langle \mathbf{0} | S_r^y(t) | \mathbf{0} \rangle = 0$ , and  $\tau[\rho^{(1)}] = 1 - 4 \langle \mathbf{0} | S_r^z(t) | \mathbf{0} \rangle^2$ . Unlike Fig. 2, the one-tangle always equals zero when  $\gamma = 0$  since the vacuum state is the ground state of the system. And the  $r^{\text{th}}$  spin will always remain in the spin-down state and will never be entangled with the other spins. For the two initial states of the system, Fig. 2(b)(c) and Fig. 3(b)(c), we find that the time evolution of the one-tangle shows similar behavior with increasing  $\gamma$ , which means the one-tangle is not sensitive to the initial state of the system when a strong anisotropy is present in the case of weak-field and intermediate regimes. This shows that the anisotropy parameter aides in the generation of entanglement in the spin chain.

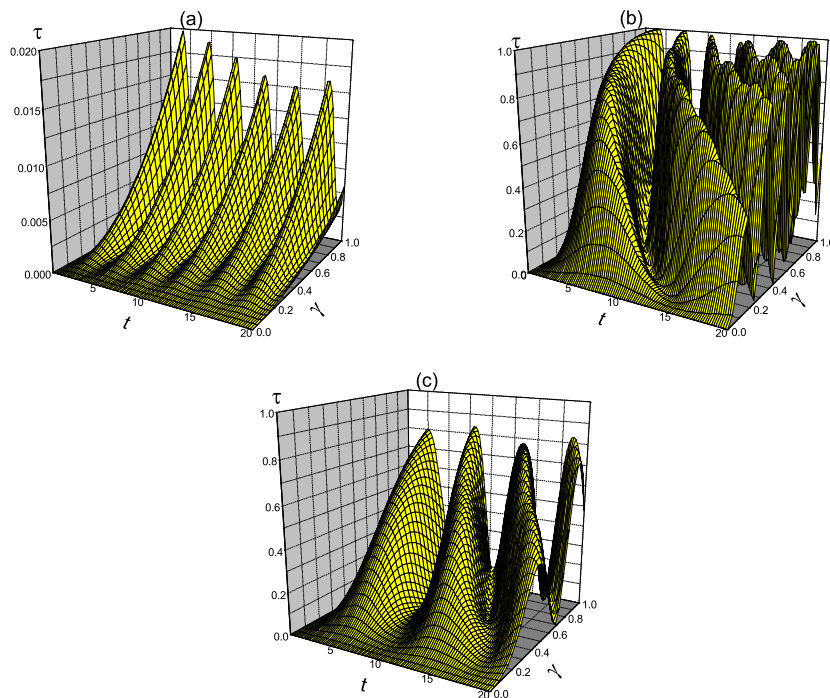


Fig. 3. Same as Fig. 2 except that the initial state is the vacuum state,  $|\mathbf{0}\rangle$ .

## 5 Conclusions

In conclusion, we have investigated quantum state transfer through an anisotropic Heisenberg XY model in a transverse field and also entanglement generation in that same system. The interest in these problems stems from the possible use of spin chains as a communication channels. We expect that a realistic ferromagnetic material would have some anisotropy and have shown that this anisotropy can have significant effects on the fidelity of state transfer as well as the entanglement in the chain.

Specifically, we have calculated the fidelity and the one-tangle, or purity, for three different cases: a weak external magnetic field, an intermediate regime, and strong external magnetic field. We found that in all three cases a relatively high fidelity can be obtained for certain times and vales of the anisotropy. However, in the intermediate regime, the oscillation of the fidelity with time is fairly low, and the peaks fairly broad. Furthermore, a fairly high fidelity is achieved in a relatively shorter time for the intermediate regime. This would imply a more reliable output, in a shorter time, when some anisotropy is present, compared to when there is none. Thus the intermediate regime presents some interesting and somewhat surprising results for state transfer and is also the best choice for reliable transfer.

We have also calculated the one-tangle, or the purity of a typical one-particle state in the chain. We began with a pure initial state and found that the stronger the anisotropy and exchange interaction, the more entanglement will be generated. This indicates that anisotropy also aides in the production of entanglement in the chain.

## ACKNOWLEDGMENTS

This material is based upon work supported by the National Science Foundation under Grant No. 0545798 to MSB. ZMW thanks the scholarship awarded by the China Scholarship Council(CSC). We gratefully acknowledge C. Allen Bishop for helpful discussions.

## References

- [1] A. K. Ekert, Phys. Rev. Lett. 67 (1991) 661.
- [2] D. Kielpinski, C. Monroe, D. J. Wineland, Nature 417 (2002) 709.

- [3] B. B. Blinov, D. L. Moehring, L.-M. Duan, C. Monroe, *Nature* 428 (2004) 153.
- [4] S. Bose, *Contemporary Physics* 48 (2007) 13.
- [5] S. Bose, *Phys. Rev. Lett.* 91 (2003) 207901.
- [6] M. Christandl, et al., *Phys. Rev. Lett.* 92 (2004) 187902.
- [7] M. Christandl, et al., *Phys. Rev. A* 71 (2005) 032312.
- [8] D. Burgarth, V. Giovannetti, S. Bose, *Phys. Rev. A* 75 (2007) 062327.
- [9] D. Burgarth, S. Bose, *Phys. Rev. A* 69 (2005) 052315.
- [10] D. Burgarth, S. Bose, *Int. J. Quan. Infor.* 4 (2006) 405.
- [11] V. Subrahmanyam, *Phys. Rev. A* 69 (2004) 034304.
- [12] V. Subrahmanyam, A. Lakshminarayan, *Phys. Lett. A* 349 (2006) 164.
- [13] Z. M. Wang, B. Shao, J. Zou, *Chinese Phys. Lett.* 24 (2007) 24.
- [14] Z. M. Wang, B. Shao, P. Chang, J. Zou, *Physica A* 387 (2008) 2197.
- [15] K. Maruyama, T. Itakac, F. Nori, *Phys. Rev. A* 75 (2007) 012325.
- [16] Z. M. Wang, B. Shao, P. Chang, J. Zou, *J. Phys. A* 40 (2007) 9067.
- [17] L. Amico, A. Osterloh, *J. Phys. A* 37 (2004) 291.
- [18] L. Amico, A. Osterloh, *Phys. Rev. A* 69 (2004) 022304.
- [19] Z. M. Wang, B. Shao, J. Zou, *Int. J. Mod. Phys. B* 22 (2008) 4853.
- [20] P. W. Anderson, *Phys. Rev.* 112 (1958) 1900.
- [21] T. J. Osborne, M. Nielsen, *Phys. Rev. A* 66 (2002) 032110.
- [22] Valerie Coffman, Joydip Kundu and William K. Wootters, Distributed entanglement, *Phys. Rev. A* 61 (2000) 052306.
- [23] R. H. Crooks, D. V. Khveshchenko, *Phys. Rev. A* 77 (2008) 062305.